Shape Effect of Crushed Sand Filler on Rheology: A Preliminary Experimental and Numerical Study

Spangenberg, Jon; Cepuritis, Rolands; Hovad, Emil; Scherer, George W.; Jacobsen, Stefan

Published in:
8th International RILEM Symposium on Self-Compacting Concrete - SCC 2016

Publication date:
2016

Document Version
Peer reviewed version

Shape effect of crushed sand filler on rheology: a preliminary experimental and numerical study

J. Spangenberg[1], R. Cepuritis[2,3], E. Hovad[1,4], G. W. Scherer[5], S. Jacobsen[2]

[1]Department of Mechanical Engineering, Technical University of Denmark, 2800 Lyngby, Denmark
[2]Department of Structural Engineering, Norwegian University of Science and Technology, 7491 Trondheim, Norway
[3]Norcem AS, R&D Department (HeidelbergCementGroup), 3950 Brevik, Norway
[4]DISA Industries A/S, 2630 Taastrup, Denmark
[5]Department of Civil and Environmental Engineering, Princeton University, Princeton, NJ 08544, USA

Abstract Two types of filler from crushed sand were mixed with cement paste with constant superplasticizer dosage per mass of cement to investigate how their shape affects the rheology. The fillers were mylonitic quartz diorite and limestone produced using Vertical Shaft Impact (VSI) crusher and air classification, and had length/thickness (L/T) aspect ratios of 2.00 and 1.82, respectively. The particles were characterized with X-ray micro-computed tomography, coupled with spherical harmonic analysis to mathematically describe the full 3-D shape of the particles, while the rheological performance was quantified with the slump flow test (i.e. mini cone). The shape effect was isolated in the experiments by the use of non-overlapping bimodal particle distributions of cement particles with a number average diameter of ≈0.01 mm and filler particles with a number average diameter of ≈0.1 mm. The two filler types were tested with a range of χ-values (volume of cement divided by total volume of solids). The flowability of the matrix increased with decreasing aspect ratios of the filler. However, the χ-value at which the maximum volume fraction threshold was obtained varied for the two filler types. Subsequently, a discrete element model was utilized to simulate the experimental data, thereby providing an initial step toward a numerical tool that can assist when proportioning self-compacting concrete with high volumes of crushed sand fines.

Keywords: *Crushed sand filler, shape effect, rheology, numerical modelling, aggregate proportioning*

Introduction

The use of crushed sand filler in concrete production is increasing due to shortage of natural aggregate deposits around the world. This development has implications for the rheological behaviour of the concrete as the crushed sand particles are less equi-dimensional than natural sand grains. The effect of particle shape has been studied by a number of researchers and found to affect rheology to various degrees depending on parameters such as length/width (L/W) ratio [1], packing ability [2], and the cubicity of the particle [3]. However, still more knowledge is needed to account for the filler shape in the design phase of concrete proportioning. Consequently, here the effects of particle shape of industrially produced crushed sand filler on flow are investigated by experiments and modelling to improve the understanding of the effect of the shape of the fines on rheology. This would allow progress in the development and optimization of crushed sand for concrete. The first part of the paper describes the methodology used to characterize the shape of the two filler types (i.e. mylonitic quartz diorite and limestone) and the procedure used to quantify the rheological behaviour of the matrix (comprising water, superplasticizer, cement, and filler). This is followed by a description of the governing equations and calibration of the discrete element method (DEM) computational fluid dynamics model that is used to mimic the experimental findings. Finally, the experimental and numerical results are analysed and the model's potential utility for proportioning self-compacting concrete (SCC) is discussed.

Experiments

The characterization of the shape of the mylonitic quartz diorite and limestone was carried out with X-ray micro-computed (μCT) tomography, coupled with spherical harmonic (SH) analysis to mathematically describe the full 3-D shape of the particles. The methodology is described in depth by Cepuritis et al. [4, 5]. In general, the procedure involved casting 5 vol% of crushed powders in epoxy and allowing hardening without segregation. After hardening, the samples were scanned using μCT equipment and complete three-dimensional renderings of the digitized particle size and shape were obtained within the limitation of the voxel size used. The SH coefficients [6] were generated using the μCT data for each of the particles. The SH approach gives an analytical, differentiable mathematical form for the particle surface and volume, so one can compute any geometric quantity of the particle that can be defined by integrals over the volume or the surface, or over points on the surface or within the volume. The average equivalent particle size was ≈0.01 mm for the cement (determined by wet-method laser diffraction) and ≈0.1 mm for the two filler types (volume equivalent particle diameter = VESD, obtained from the μCT SH analysis), see Fig. 1. The mean aspect ratios (length/thickness =L/T and length/width=L/W) describing mutually

orthogonal dimensions which form a box that just encloses a particle were the following for the two filler fractions:

- Mylonitic quartz diorite: L/T = 2.00 and L/W = 1.38 as number-weighted mean values and L/T = 2.09 and L/W = 1.39 as volume-weighted mean values;
- Limestone: L/T = 1.82 and L/W = 1.32 as number-weighted mean values and L/T = 1.90 and L/W = 1.30 as volume-weighted mean values.

The L/T aspect ratios of separate bins of particles from the mylonitic quartz diorite and limestone samples are provided in Fig. 2. Examples of 3-D images (created with Virtual Reality Modelling Language, VRML) based on the SH method of approximating the shape [6] of the two filler types, having the same aspect ratios as introduced above, are shown in Fig. 3.

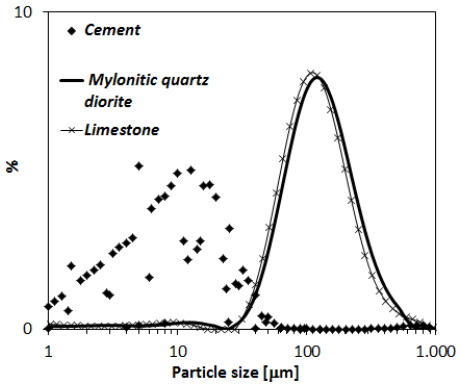

Figure 1. The mass- (or volume-) weighted particle size distributions of the cement, mylonitic quartz diorite and limestone.

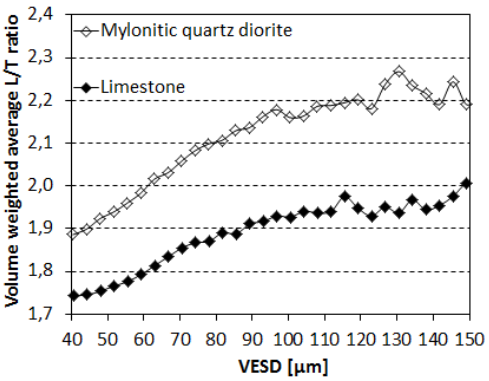

Figure 2. The volume weighted average L/T aspect ratio as a function of the size of the two fillers. Size given as volume equivalent sphere diameter (VESD). The average L/T for each size is based on a high enough number of particles to give converging L/T [5].

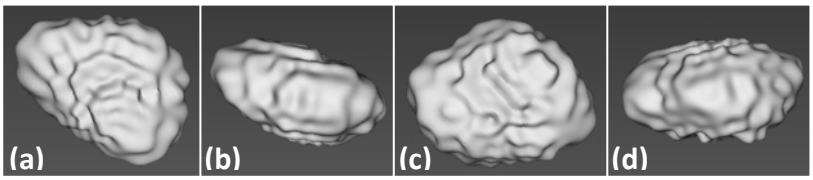

Figure 3. VRML images of particles based on the results from μCT scanning and SH analysis; (a), (b) two views of a mylonitic quartz diorite particle of VESD = 52 μm, L/T = 2.00 and L/W = 1.38; (c), (d) two views of a limestone particle of VESD = 52 μm, L/T = 1.82 and L/W = 1.32. The number-weighted particle aspect ratios represents the mean values of the whole powder samples, as introduced above.

The density measurements of the three particles were performed with He-pycnometry. The density was 3130 kg/m^3 for the cement and 2770 kg/m^3 for both fillers. Measurements of compacted dry packing gave slightly lower values (0.526) for T1 Quartz than for T6 Limestone (0.536) as expected from differences in average L/T and similar PSD. The procedure used to mix the matrix was developed by Ng et al. [7] and consists of five steps: 1. dry mixing the cement and the filler in question; 2. adding the water and superplastisizer (10 g per kg cement); 3. mixing the matrix for 2 minutes; 4. pausing the mixing for 1 minute; 5. mixing the matrix for additional 2 minutes. The mixing was conducted with a drill machine with a whisk-shaped drill in a plastic cylinder with a diameter of 11 cm and a height of 29.7 cm. The rheological characterization of the matrix was carried out with the slump flow test. The mini cone used for the test had a height of 73 mm, a lower diameter of 89 mm, and an upper diameter of 39 mm, making the cone of similar size as the one used by Roussel et al. [8] when relating the mini-cone test to Abrams cone test.

Numerical model

In this work, the discrete element method (DEM) was used to simulate the flow of the matrix. The DEM method has previously been utilized to emulate the non-Newtonian flow behaviour of fresh cementitious materials in the J-ring test [9], slump flow test [10], and LCPC-box test [11]. The DEM method is an approach where particles are included for discretization purposes (e.g. to describe the flow of a fluid in which the particle could be seen as a virtual particle) and/or for representation of aggregates. In our numerical model, particles were used to discretize the flow of the water as well the movement of cement and filler particles. The model was developed in the commercial software STAR-CCM+. The governing equations that were solved to obtain the flow behaviour of all three phases of the matrix are described in the following.

Normal direction. Hertzian contact mechanics was used [12]. The normal interaction force between the particles i and j is given by

$$\mathbf{F}_{n_{ij}} = \mathbf{n}_{ij} K_n \delta_{n_{ij}}^{3/2} - N_n \mathbf{v}_{n_{ij}}, \tag{1}$$

where $\mathbf{n}_{ij}$ is the normal vector of the plane of the two particles, K_n is the stiffness in the normal direction, $\delta_{n_{ij}}$ is the normal overlap, N_n is the normal damping coefficient, and $\mathbf{v}_{n_{ij}}$ is the normal relative velocity.

Tangential direction. A simplified Mindlin model was used [13]. The tangential force between the particles i and j is defined as

$$\mathbf{F}_{t_{ij}} = K_t \frac{\mathbf{t}_{ij}}{\left|\mathbf{t}_{ij}\right|} \delta_{t_{ij}}^{3/2} - N_t \mathbf{v}_{t_{ij}}, \tag{2}$$

where subscript t denotes the tangential direction and $\mathbf{t}_{ij}$ is the tangential displacement given by the product of the tangential relative velocity and the time increment.

Rolling resistance. The torque from the rolling resistance that counteracts the tangential force is defined as

$$\mathbf{T}_{rol} = -\frac{\boldsymbol{\omega}_{rel}}{\left|\boldsymbol{\omega}_{rel}\right|} \mu_r R_{eq} \left|\mathbf{F}_{n_{ij}}\right|, \tag{3}$$

where $\boldsymbol{\omega}_{rel}$ is the relative rotation between the particle i and j, μ_r is coefficient of rolling friction, and R_{eq} is equivalent radius.

Cohesion force. The cohesion force is obtained with the Johnson-Kendall-Roberts model with the factor of -1.5,

$$\mathbf{F}_{coh} = -1.5 \mathbf{n}_{ij} \pi R_{min} \mathrm{W}, \tag{4}$$

where R_{min} is the radius of the smallest particle in contact and W is the constant work of cohesion.

Summing forces and torques. The total force on the particle is given by

$$\mathbf{F}_i^{tot} = m_i \mathbf{g} + \sum_j \left(\mathbf{F}_{n_{ij}} + \mathbf{F}_{t_{ij}} + \mathbf{F}_{coh} \right), \tag{5}$$

where m_i is the mass of particle i and $\mathbf{g}$ is gravity. The total torque is given by

$$\mathbf{T}_i^{tot} = -R_i \sum_j \left(\mathbf{n}_{ij} \times \mathbf{F}_{t_{ij}} \right) + \sum_j \left(\mathbf{T}_{rol} \right), \tag{6}$$

where R_i is the radius of particle i. From Eqns. (5) and (6), the acceleration, velocity and position are calculated incrementally for each time step by Newtons 2nd law.

The water and cement particles were both simulated as spheres with a diameter of 0.0025 m, while the fillers where modelled by combining three spheres with a diameter of 0.005 m in order to obtain their individual aspect ratio. These choices had the following implications: 1. the hydrodynamic effect of the water decreased, as the water was modelled as hard spheres each representing a large group of water molecules; 2. the cement particles would not as easily flow between the larger particles as the size ratio (size of cement particle divided by size of the filler) was less than 1:10; 3. the number of cement and filler particle interactions decreased as the cement and filler were modelled larger than their real size. However, in spite of these simplifications, we believe the model mimics the matrix in a sensible way. In Fig. 5, the particle that represents the mylonitic quartz diorite filler is shown (aspect ratio 2.00). The total number of particles used in each simulation was ~20,000 and the calculation time was a couple of days.

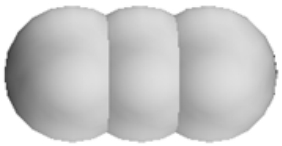

Figure 5: The particle that represents the mylonitic quartz diorite filler.

The simulation of the slump flow test was carried out by randomly filling the cone geometry with particles that represented the three phases, see Fig. 6. Subsequently, the cone geometry constraint was removed and the matrix was able to deform. Finally, the slump was computed when the matrix stopped flowing.

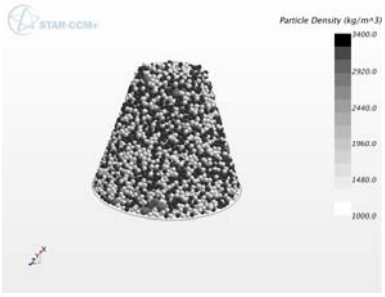

Figure 6. The initial condition for the numerical model. The three phases are water, cement, and mylonitic quartz diorite.

Model Calibration

The DEM approach requires a large set of material parameters such as a rolling resistance and cohesion value describing the interaction between two particles of the same phase, as well as the interaction between two different phases. In this study, these material parameters were obtained with an inverse analysis. Firstly, the rolling resistance and cohesion value were obtained for water and cement by fitting the numerically predicted slump to an experimental result where only those two phases were used. In this experiment, the volume fraction of the cement was 0.416. Secondly, the material parameters were acquired for each type of filler by a similar procedure, now keeping constant the properties of the water and cement and only calibrating the filler parameters. In this experiment, the total volume fraction of solids was 0.5 and the volume of cement divided with the total volume of solids, χ, was 0.1. After the calibration was performed, the rest of the experiments was simulated only by changing the volume fraction of the phases. The rolling resistance for all three phases was modelled with a coefficient of 0.2. In Table I, the cohesion parameter for the cement and fillers is shown.

Table I. The DEM cohesion parameter for cement, mylonitic quartz diorite, and limestone.

Material	Interaction	Cohesion [J/m^2]
Cement	Water	0.51
	Cement	
Mylonitic quartz diorite	Water	4.10
	Cement	
	Mylonitic quartz diorite	
Limestone	Water	0.45
	Cement	
	Limestone	

Results

In Fig. 7, an example of the experimental and numerical slump flow test is illustrated. In this test, the matrix consisted of water, cement, and mylonitic quartz diorite. The volume fraction of solids in the matrix was 0.533 and χ was 0.35. The slump was found to be 205 mm and 195 mm in the experiment and simulation, respectively. Note that some of the simulated particles are detached from the bulk of the simulated material. This artefact is a consequence of the relative coarse discretization and is disregarded when calculating the numerical slump.

Figure 7. (left) Experimental and (right) numerical slump flow test.

In Fig. 8(left), the experimental slump results for the mylonitic quartz diorite and limestone based matrices are shown for different volume fraction of solids when using χ=0.35. The results illustrate that for a given volume fraction with this χ-value, the limestone based matrix is more flowable than the mylonitic quartz diorite based matrix, which is expected, since the mylonitic quartz diorite has a greater L/T aspect ratio than the limestone. In addition, it is seen that the results can be approximated with a linear regression line and that this relationship can be used to approximate the volume fraction at which the matrix for the given χ-value does not flow (i.e. the slump is equal to the bottom diameter of the mini-cone). This volume fraction is here referred to as the volume fraction threshold. Comparing the experimental and numerical results for the limestone based matrix with χ=0.35, see Fig. 8(right), the predictions of the numerical model are within 10% of the experiment values, but the slope (based on only 3 points) appears to be quite different resulting in a larger volume fraction threshold for the numerical results. A similar analysis to find experimental and numerical volume fraction thresholds for the two types of filler with χ=0.1, 0.4 and 1 is shown in Fig. 9. The experimental results indicate that the maximum volume fraction threshold is found at increasing χ-values when the aspect ratio of the filler increases. It is interesting to see that this trend is observed for aspect ratios that vary by less than 10 %, which emphasises the importance of taking the shape effect of the filler into account when proportioning SCC. The numerical predictions differ by 4-10 % (relative) from the experimental values, which is not bad, considering that the

cement and filler phases in the numerical model were calibrated for a single volume fraction at χ=1 and 0.1, respectively. In general, the numerical solution overestimates the volume fraction threshold and its gradient from χ = 0.35 to 0.4 (in one case it predicts a wrong gradient), but it correctly accounts for the relative positions of the curves for the two aspect ratios. The discrepancies might be decreased by refining the discretization and/or exploiting other interactions models.

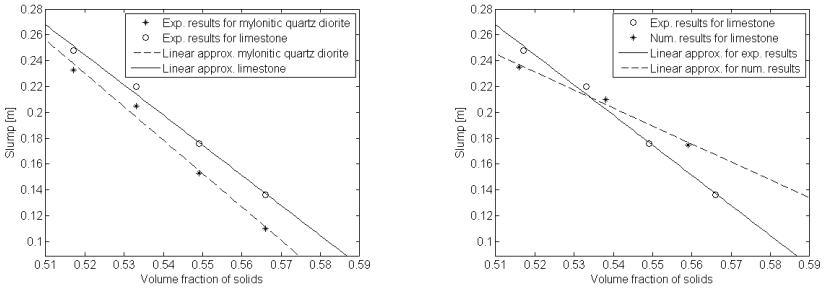

Figure 8. (left) Experimental slump results and linear approximation for the mylonitic quartz diorite and limestone based matrices at different volume fraction of solids when using χ=0.35. (right) Experimental and numerical slump results and linear approximation for the limestone based matrices at different volume fraction of solids when using χ=0.35.

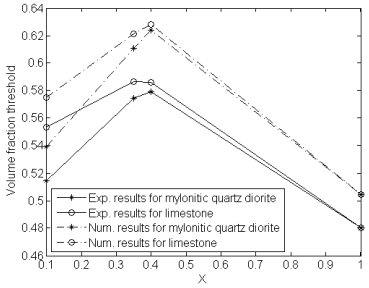

Figure 9. Experimental and numerical volume fraction thresholds as a function of χ for the two types of filler.

Conclusion

In this paper, we isolated the shape effect of crushed sand fillers on rheology by the use of non-overlapping bimodal particle distributions of cement and filler. The experimental findings showed that the flowability of the matrix decreased with increasing aspect ratio of the filler, and that the maximum volume fraction threshold varied for the two types of filler. We used a DEM model to simulate the slump flow tests and obtained numerical predictions that were within 10 % of the

experimental results. The discrepancy resulted in a slight overestimation of the volume fraction threshold by the model. Nevertheless, the numerical results seem promising and we intend to further develop the DEM model by refining the discretization and exploring other interaction models.

Acknowledgements

The authors would like to thank Dr. Edward J. Garboczi of NIST for help with the μCT SH analysis and Dr. Ya Peng for helping with the rheology measurements. We also acknowledge the support of the Scientific Research Council on Technology and Production Sciences a part of the Danish Council for Independent Research (Contract No. 4005-00381), and the Norwegian Research Council (Contract No. 247619/O30).

References

[1] Douglas, J. F., Garboczi, E. (1995), Adv. Chem. Phys., vol. XCI, pp. 85-153.
[2] Larrard, F. de, (1999), E & FN Spon, London.
[3] Andus, D. J., Hassan, A. M., Garboczi, E. J., Douglas, J. F. (2015), Soft Mattter, vol. 11, n. 17, pp. 3360-3366.
[4] Cepuritis, R., Garboczi, E. J., Jacobsen, S., and Snyder, K., *Powder Technol.*, (submitted).
[5] Cepuritis, R., Garboczi, E. J., and Jacobsen, S., *Cem. Concr. Comp.*, (submitted).
[6] Garboczi, E. (2002), *Cem. Concr. Res.*, vol. 32, pp. 1621-1638.
[7] Ng., S., Mujica, H., and Smeplass, S. (2014), *Nord. Concr. Res.*, vol. 51, no. 3, pp. 15-28.
[8] Roussel, N., Stefani, C., and Leroy, R. (2005), Cem. Concr. Res. vol. 35, pp. 817-822.
[9] Gram, A. (2009), Licentiate thesis, Royal Institute of Technology (KTH)
[10] Mechtcherine, V., Gram, A., Krenzer, K., Schwabe, J-H., Shyshko, S., Roussel, N. (2014), *Mater. Struct*, vol. 47, pp. 615-630.
[11] Roussel, N., Gram, A., Cremonesi, M., Ferrara, L., Krenzer, K., Mechtcherine, V., Shyshko, S., Skocek, J., Spangenberg, J., Svec, O., Thrane, L. N., Vasilic, K. (2016), *Cem. Concr. Res.* vol. 79, pp. 265-271.
[12] Hertz, H. (1881), *J. Angew. Math.*, vol. 171, pp. 156-171.
[13] Tsuji, Y., Tanaka, T., Ishida, T. (1992), *Powder Technol.* vol. 71, pp. 239-250.